



CHALMERS
UNIVERSITY OF TECHNOLOGY

Surface instability detection in highly-filled biocomposites from inline imaging during extrusion

Downloaded from: <https://research.chalmers.se>, 2025-06-08 01:36 UTC

Citation for the original published paper (version of record):

Pashazadehgaznagh, S., Moberg, T., Brodin, A. et al (2023). Surface instability detection in highly-filled biocomposites from inline imaging during extrusion. AIP Conference Proceedings, 2997. <http://dx.doi.org/10.1063/5.0159814>

N.B. When citing this work, cite the original published paper.

RESEARCH ARTICLE | JUNE 08 2023

Surface instability detection in highly-filled biocomposites from inline imaging during extrusion

Sajjad Pashazadeh ; Tobias Moberg; Anders Brolin; Roland Kádár

AIP Conf. Proc. 2997, 020008 (2023)

<https://doi.org/10.1063/5.0159814>



View
Online



Export
Citation

Surface Instability Detection in Highly-Filled Biocomposites from Inline Imaging during Extrusion

Sajjad Pashazadeh^{1, a)} Tobias Moberg^{2, b)} Anders Brodin^{3, c)} Roland Kádár^{1,4,5, d)}

¹*Chalmers University of Technology, Department of Industrial and Materials Science, Gothenburg, SE 412 96, Sweden*

²*Stora Enso AB, Circular Solutions, Packaging Solutions, Hylte Mill, SE 314 81, Hyltebruk, Sweden*

³*Stora Enso AB, Group Innovation and R&D, Karlstad Research Center, SE 650 09, Karlstad, Sweden*

⁴*FibRe-Centre for Lignocellulose-based Thermoplastics, Department of Chemistry and Chemical Engineering, Chalmers University of Technology, Gothenburg, SE 412 96, Sweden*

⁵*Wallenberg Wood Science Centre, Chalmers University of Technology, Gothenburg, SE 412 96, Sweden*

^{a)} Corresponding author: sajjadp@chalmers.se

^{b)} tobias.moberg@storaenso.com

^{c)} anders.brolin@storaenso.com

^{d)} roland.kadar@chalmers.se

Abstract. The processing of wood fiber biocomposites, and in particular, the extrusion, is accompanied by multiple challenges, among which agglomeration, entanglement, slip, or surface instabilities being the most common ones. In the current work, we focus on the dynamics of surface instabilities during the single screw extrusion of highly filled wood fiber biocomposites. The biocomposites are polypropylene based with up to 40 wt% wood fiber content of custom compositions based on the commercial-grade by Stora Enso. To detect and quantify the dynamics of surface instabilities, inline image analysis was applied using an optical visualization system positioned at the die exit. Therefrom, space-time diagrams were constructed, and after that, via 2D-Fourier transform analysis, the spatio-temporal spectral dynamics of the surface instabilities were determined as a function of the die (apparent) shear rate. The spectral dynamics show that melt instabilities of 40 wt% for example, detected via their characteristic (temporal) frequency and (spatial) wavenumber, dissipate with increasing the shear rate, such that at shear rates above ca. 90 1/s, no characteristic frequency and wavenumber can be distinguished i.e. instabilities can no longer be observed on the surface of the extrudates.

INTRODUCTION

Even though using wood fiber composites (WPCs) can improve mechanical properties, processing them has some specific challenges. From a processing point of view, the surface quality of the final product is a crucial factor. Numerous studies have been devoted to investigating surface instabilities in neat polymers. While their surface quality tends to be smooth at low screw speeds (shear rates), different types of surface irregularities, such as sharkskin or slip-stick, depending on the type of the polymer and its molecular weight, emerge with increasing shear rate. At very high shear rates, gross melt fracture instabilities can also be observed. More information about extrusion instabilities of pure polymers can be found in several recent studies [1-7]. Distinct from the instabilities mentioned earlier, another kind of surface irregularity can be observed in WPCs, referred to as "surface tearing" (ST) instability. This type of instability was observed for the first time by Goettler et al. [8] in short, cellulose fiber/rubber composites. There are several approaches to improving surface quality, among which promoting wall slip velocity is an effective one. The slip velocity of WPCs can be increased either by increasing wood filler concentration or shear rate. Many other factors can impact the surface quality of WPC, starting from additives, lubricants, and coupling agents to flow geometry and processing parameters such as die aspect ratio, shear rate, and temperature. Sufficiently high shear rates, together with the high wood contents, can lead to higher wall slip velocity and thus reduce surface tearing instabilities [9-11].

Extrusion melt flow instabilities, performed using capillary rheometers, in Polyethylene (PE) and Polypropylene (PP) polymers with up to 30 - 60 wt% Maple wood flour have been investigated by Histrov et al. [9]. Their work pointed to an intensified shear tearing upon the inclusion of wood flour content up to 50 wt%. However, at highly filled systems with more than 60 wt% of filler, surface tearing was decreased due to the slip and plug flow. In another study by Histrov et al. [10], the authors reported a sharp increase in the slip velocity of HDPE/wood flour composite at highly filled WPCs of 60 - 70 wt% filler content using a capillary die with $L/D = 16$. As a result, they concluded that smoother surfaces can be achieved for highly filled composites (60 - 70 wt%). The same authors [12] explored the rheological response of PE/wood flour composites from capillary rheometry. Their findings point to the suppression of surface tearing instabilities with capillary rheometry at high aspect ratios (L/D). Nevertheless, at a fixed L/D , the increase in the die diameter results in more intense surface instabilities.

Present Study

In this study, we show for the first time [13, 14] the detection and spatio-temporal dynamics of wood fiber biocomposite melt surface instabilities during single-screw extrusion using an inline optical visualization. With the help of spectral dynamics, the onset, peak, and decay of instabilities can be easily mapped as function of filler concentration and shear rate.

Materials and Method

Commercial biocomposite with 40 wt% wood fiber content supplied by StoraEnso was used in this study as an example and to introduce the method. Pellets were kept at 90 °C in a convection oven for five days for drying prior to the experiments. The dried pellets were then fed to a Brabender 19/25D (barrel diameter $D = 19$ mm, barrel length $L = 25D$) single screw extruder equipped with a compression screw (ratio of 3/1). A slit die (rectangular cross-section) with length \times width \times thickness of 132 \times 20 \times 2 mm was used in the experiments. To measure the pressure two melt pressure transducers (Terwin instrumnets) were used. The setup schematic is shown in Fig. 1. The temperature from the feeding zone toward the die were set respectively to 150, 170, 190, and 190°C. The screw speed (n) was set from 0 to 150 rpm with a ramp rate of $dn/dt = 0.1$ rpm/s, where t represents the time.

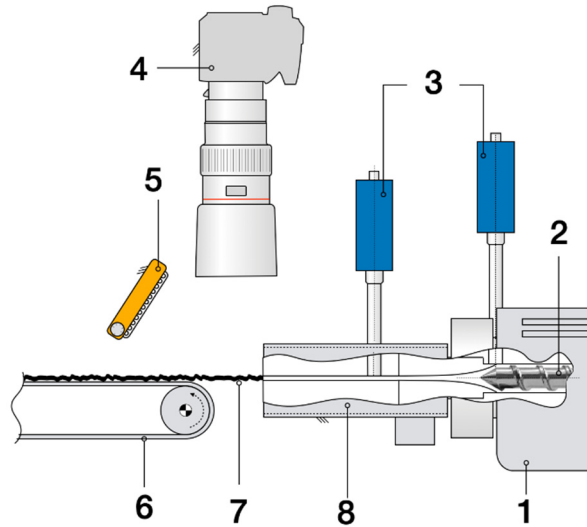


FIGURE 1. Schematic of the experimental setup: 1 Brabender 19/25D single screw extruder, 2 compression screw (C3:1), 3 melt pressure transducer, 4 Canon EOS 90D DSLR camera, 5 LED 850 lx lights, 6 conveyor belt, 7 Extrudate, 8 slit die.

The extrudate at the die exit was video recorded using a Canon EOS 90D DSLR camera in full HD format (1920 \times 1080 pixels) at 100 fps (frames per second). For data analysis, a space-time diagram of the recorded video was constructed [7, 15], and subsequently 2D Fourier transform was applied on a moving window on the space-time diagram. The Fourier transform of a 2D function $f_j(t, x_2)$ is

$$F_j(t, x_2) = \int_{-\infty}^{\infty} \int_{-\infty}^{\infty} f_j(t, x_2) e^{-i(\omega \cdot t, k \cdot x_2)} dt dx_2$$

where t and x_2 correspond to the x, y -axes of a moving frame j along a space-time diagram. Thus, for supercritical extrusion flows (non-smooth extrudates) a pair of temporal and spatial frequencies $(\omega, k)_j$ characterizes the visual pattern of the extrudate distortions. Their dynamics can then be determined based on their variation with the moving window j along the space-time diagram in the form of temporal and spatial spectrograms.

Results

An example of space-time diagram for a 40 wt% biocomposite, temporal and spatial spectrograms represented as function of time, as well as apparent shear rate ($\dot{\gamma}_a$) are shown in Fig. 2. The latter were calculated from the screw speed (n) based on volumetric flow rate conservation [16]. The y -axes in the space-time diagram, temporal, and spatial spectrograms, stand for the width of the slit die (distance mm equivalent to x_2 in Eq. (1)). The colormaps are adjusted relatively to the maximum and minimum intensity of $F(t, x_2)$, where the dark blue and dark red colors correspond to the minimum and maximum intensity on both spectrograms, Fig. 2b,c. Thus, distinct peaks in frequency and wavenumber can be readily identified as the characteristic temporal frequency and wavenumber of the ST instability mode, $(\omega, k)_{ST}$. Due to intensive surface tearing and low shear rates, the frequency and wavenumber show high intensity (dark red) at $5 < \dot{\gamma}_a < 70$ 1/s. With increasing shear rate, the temporal spectrogram, Fig. 2b, clearly shows a decay in the intensity of the characteristic frequency and that the decay of surface tearing is accompanied by the broadening of the characteristic peak frequencies. This can be visually observed on the inline and offline images in Fig. 3.

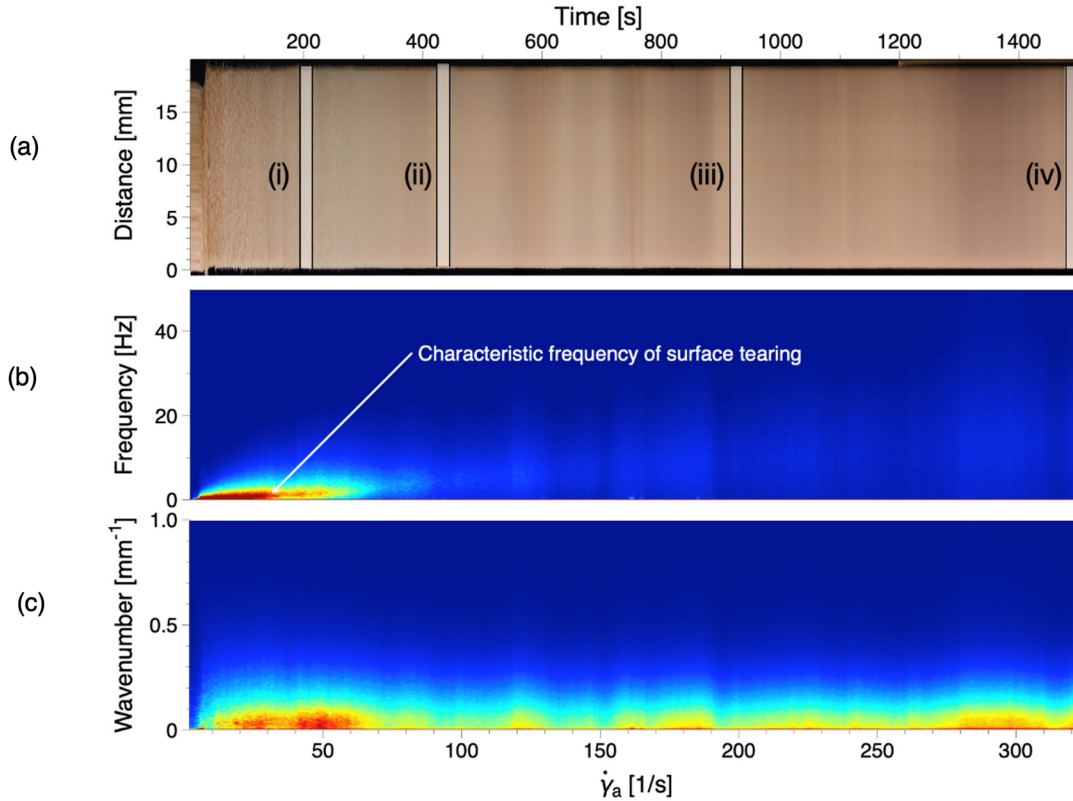


FIGURE 2. Spectral dynamics of 40 wt% at 190°C: a) Space-time diagram, b) (Temporal) Frequency spectrogram, and c) (spatial) wavenumber spectrogram.

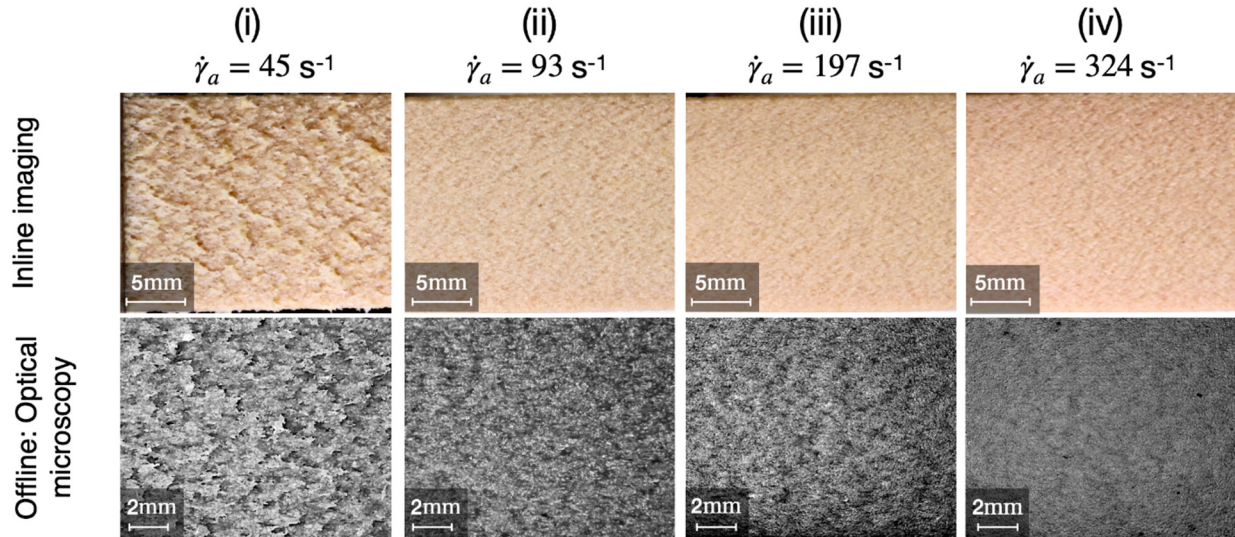


FIGURE 3. Inline and offline images of extrudate at four different shear rates of 45, 93, 197, and 324 1/s, which correspond to the (i), (ii), (iii), and (iv), in Fig. 2a.

In detail, Fig. 4a shows the frequency spectra at four different shear rates of 45, 93, 197, and 324 1/s, which correspond to the four sets of images in Fig. 3 (i), (ii), (iii), and (iv), respectively. Fig. 4a confirms that at the lower shear rate, the characteristic frequency peaks are sharp and narrow, but with increasing shear rate, intensity peaks decrease and become broader. The ratio of maximum characteristic frequency peak to minimum intensities is illustrated in Fig. 4b, and we can consider it as a criterion to see the decay of ST in detail, where we can observe signal-to-noise (S/N) ratio as a function of apparent shear rate. Fig. 4b shows an exponential decay of S/N values, and at $\dot{\gamma}_a > 200$ 1/s, it becomes almost constant. Concomitantly, a decay in characteristic wavenumber, Fig. 2c, is also recorded, however, no clear surface pattern characteristic wavenumbers could be distinguished $\dot{\gamma}_a > 70$ 1/s. We have shown through surface profilometry that the broad weak temporal spectra corresponds to the surface roughness of the extrudates in the absence of surface instabilities [13, 14].

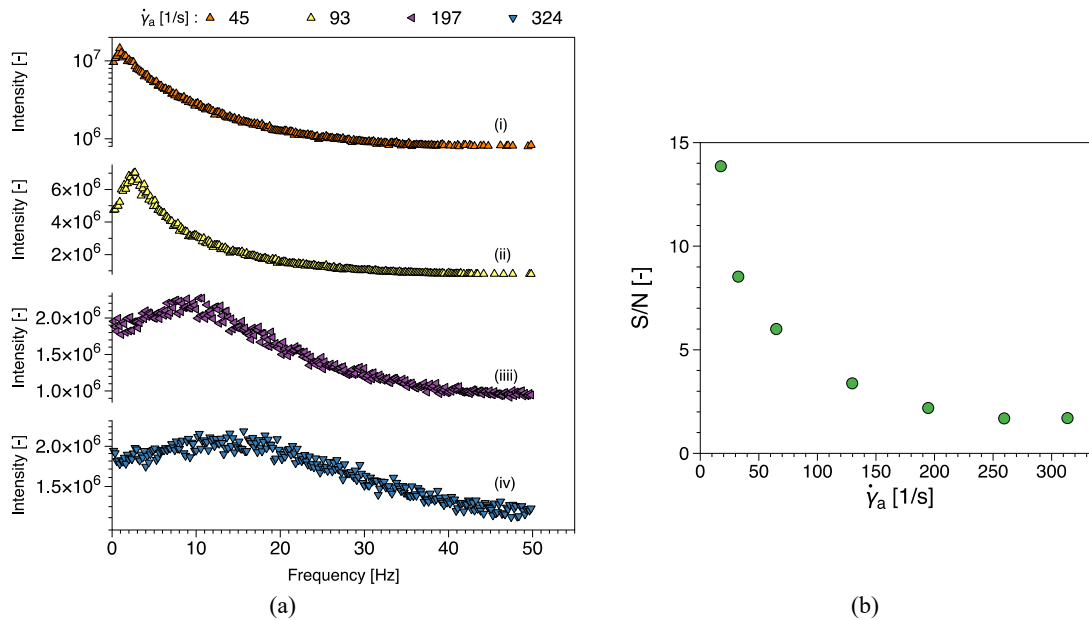


FIGURE 4. a) Frequency spectra at four different shear rates of 45, 93, 197, 324 1/s, b) Signal to noise vs apparent shear rate from the data in Fig. a.

Fig. 4a, and b are in good agreement with inline and offline images shown in Fig. 3. Both sets of images show that melt flow of 40 wt% biocomposite at low shear rates ($\dot{\gamma}_a < 50$ 1/s) shows intensive ST instabilities, however, by increasing the shear rate, the ST start to dissipate, where approximately at shear rates $\dot{\gamma}_a > 90$ 1/s, the extrudate surface are visibly smoother. Similar trends are also observed in the previous studies with wood flour composites, see [9-12]; interestingly, this phenomenon in contrary to the melt flow instability of neat polymers. The extrusion flow of unfilled polymers exhibits a smooth surface (no instability) at low shear rates, followed by the appearance of instabilities such as sharkskin, stick-slip, and gross melt fracture at higher shear rates.

SUMMARY AND CONCLUSIONS

In this study, we focus on the dynamics of surface instabilities during the (single-screw) extrusion of wood fiber biocomposites. The biocomposite was polypropylene based with up to 40 wt% wood fiber content. Inline image analysis was applied using an optical visualization system positioned at the die exit. Therefrom, space-time diagrams were constructed, and after that, via 2D-Fourier transform analysis, the temporal and spatial characteristic periodicities were quantified. Spectrograms showed surface tearing instability occurred from the lowest (stable) shear rates investigated, and by increasing the shear rate, the instabilities started to decay. Spectral evolution spectrums correlate well with inline and offline images. A mechanism for surface tearing has been previously proposed as a result of extensional rates at the die exit due to swelling and low extensional leading to surface cracks [9], similar to the sharkskin instability but enhanced by poor adhesion between wood fiber and matrix. Polypropylene thus tends to swell at the die exit; however, the presence of fillers reduces swelling, and since there is poor bonding between the wood fibers and polymer, relatively large surface cracks occur. The reason behind surface tearing instabilities decay is wall slip. Wall slip of wood fiber composites is common and has been previously observed [10].

ACKNOWLEDGMENTS

This work has been carried out within the Biocomposite program generously funded by the Knut and Alice Wallenberg foundation (Dnr. KAW 2018.0451). Stora Enso Oyj is gratefully acknowledged for financial support.

REFERENCES

1. den Doelder, C.F.J., *Design and implementation of polymer melt fracture models*. 1999.
2. A. Gansen, et al., *J. Appl. Polym. Sci.* **137**, 48806 (2020).
3. R. Koopmans, J. Den Doelder and J. Molenaar, *Polymer melt fracture*. 2010: CRC Press.
4. I. F. Naue, R. Kádár and M. Wilhelm, *Macromolecular Materials and Engineering*, **300**, 1141-1152 (2015).
5. K. F. Ratzsch, et al., *Macromolecular Materials and Engineering*, **298**, 1124-1132 (2013).
6. C. K. Georgantopoulos, et al., *Macromolecular Materials and Engineering*, **306**, 2000801 (2021).
7. C. K. Georgantopoulos, et al., *Physics of Fluids*, **33**, 093108 (2021).
8. L- Goettler, J. Sezna, and P. DiMauro, *Rubber World*, **187**, HS-033 913 (1982).
9. V. Hristov, *Composite Interfaces*, **16**, 731-750 (2009).
10. V. Hristov, E. Takacs and J. Vlachopoulos, *Polymer Engineering & Science*, **46**, 1204-1214 (2006).
11. V. Hristov and J. Vlachopoulos, *Polymer composites*, **29**, 831-839 (2008).
12. V. Hristov and J. Vlachopoulos, *Rheologica acta* **46**, 773-783 (2007).
13. S. Pashazadeh, *Mapping surface defects in highly-filled wood fiber polymer composite extrusion from inline spectral analysis*. manuscript in review, 2023.
14. S. Pashazadeh, *Licentiate thesis, " Highly filled biocomposites: processing, modlling, and characterization"*, in *Department of Industrial and material science (IMS)*, Chalmers University of Technology Editor. 2022 October.
15. R. Kádár, I. F. Naue and M. Wilhelm, *Simultaneous in-situ analysis of instabilities and first normal stress difference during polymer melt extrusion flows*. Annu. Trans. of the Nordic Rheol. Soc, 2014. **22**: p. 153-160.
16. Giles Jr, H. F., E.M. Mount III, and J.R. Wagner Jr, *Extrusion: the definitive processing guide and handbook*. 2004: William Andrew.